Available online at www.sciencedirect.com

ScienceDirect

Russian Geology and Geophysics 57 (2016) 617–628

RUSSIAN GEOLOGY AND GEOPHYSICS

www.elsevier.com/locate/rgg

Vertical and lateral spreading of highly mineralized acid drainage solutions (*Ur dump, Salair*): electrical resistivity tomography and hydrogeochemical data

V.V. Olenchenko [a,b,*], D.O. Kucher [a], S.B. Bortnikova [a], O.L. Gas'kova [b,c], A.V. Edelev [a], M.P. Gora [b]

[a] *A.A. Trofimuk Institute of Petroleum Geology and Geophysics, Siberian Branch of the Russian Academy of Sciences, pr. Akademika Koptyuga 3, Novosibirsk, 630090, Russia*

[b] *Novosibirsk State University, ul. Pirogova 2, Novosibirsk, 630090, Russia*

[c] *V.S. Sobolev Institute of Geology and Mineralogy, Siberian Branch of the Russian Academy of Sciences, pr. Akademika Koptyuga 3, Novosibirsk, 630090, Russia*

Received 16 March 2015; accepted 28 May 2015

Abstract

Combined geophysical and geochemical investigations of drainage streams from sulfide-containing waste dumps of the Novo-Urskoe deposit allow determining two directions of highly mineralized toxic solutions. Surface drainage stream flows over the natural slope of the valley. In addition, along the natural fault, vertical penetration of drainage solutions into groundwater occurs to a depth of 20 m. Based on geophysical-data interpretation, we assume that penetration of solutions into geologic environment leads to their dilution by groundwater, followed by a six-fold decrease in total mineralization.

Keywords: acid drainage; heavy metals; electrical resistivity tomography; 3D model

Introduction

The current exposure of dump rocks, ore tailings, and metal industry slags to oxidation and transport factors has radically changed the geochemical pattern and history of mining regions not only in Russia but also worldwide. The discovery of toxic heavy-metal anomalies near enrichment plants in the 1970s (Blair et al., 1980; Boorman and Watson, 1976) started a new epoch in the development of geosciences: The priorities of both applied and fundamental studies were given to the research into the consequences of man's activity in the field of mining. Formation and spreading of acid drainage solutions from tailings of sulfide and sulfide-bearing ores is the problem actively discussed in the world literature. Water transport of potentially toxic elements from waste storages gradually becomes a large-scale process because of the destruction of the mineral matrix of tailings and the passing of elements into mobile forms. Formation of highly mineralized solutions within the dumps and the direction of their subsequent migration in the environment are the issues, which have to be solved for working out protective measures against the harmful effect of acid drainage water. Surface water flows permit a more or less reliable tracing of the migration of metals discharged from dumps (Sainz et al., 2004), whereas the relationship of groundwater contamination with aquifers is determined by borehole sampling (Kargar et al., 2012; Oilas et al., 2012; Spiridonov et al., 2014) or geophysical sounding (Ayolabi et al., 2013; Bortnikova et al., 2011; Yuval and Oldenburg, 1996). In Russia, there are hundreds of abandoned, existing, and appearing mining and mineral processing industry waste storages. Part of the dumps is an open source of technogenic environment pollution favored by the hydrogeologic conditions. Their main agents of pollutant transfer are water draining through the dumps (surface drainage streams) and flows filtered into aquifers in different directions (depending on the structural peculiarities of the geologic environment). Today, many types of tailings storages are under thorough control and require a search for the ways of remediation of environment- and public-hazardous objects.

We determined the compositions and directions of drainage solutions in the geologic environment for understanding the

* Corresponding author.
E-mail address: OlenchenkoVV@ipgg.sbras.ru (V.V. Olenchenko)

1068-7971/$ - see front matter © 2016, V.S. Sobolev IGM, Siberian Branch of the RAS. Published by Elsevier B.V. All rights reserved.
http://dx.doi.org/10.1016/j.rgg.2015.05.014

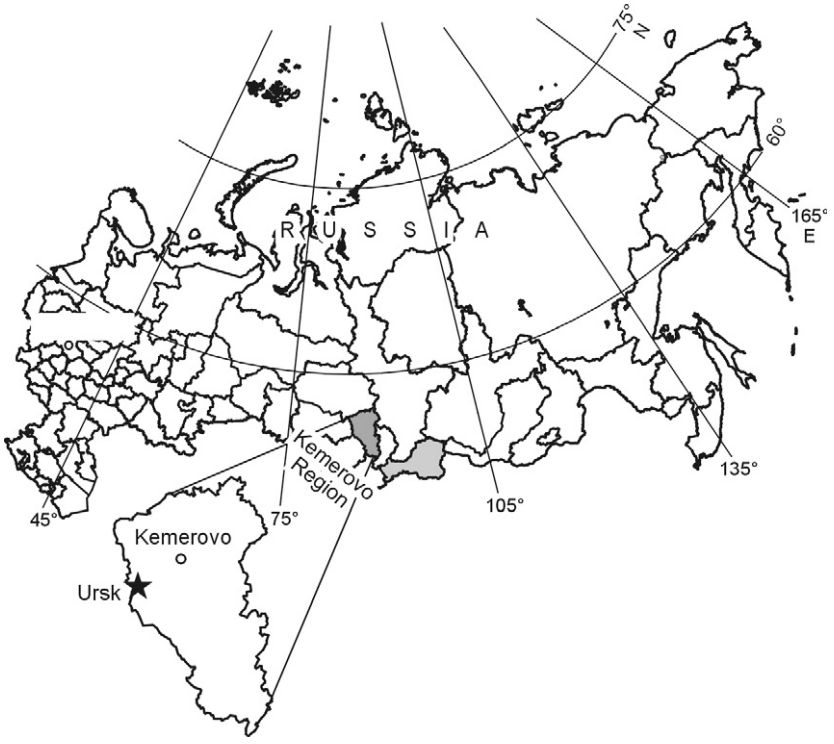

Fig. 1. Geographic location of the object of study (asterisked).

genesis of drainage flows from bulk dumps. Geochemical sampling and geophysical sounding were performed at the dump of the Novo-Urskoe deposit (Kemerovo Region, Ursk Village, Fig. 1). We have revealed an internal zoning of the dump, reflecting the spreading of highly mineralized solutions in the interstices, and have shown the spreading of drainage flows from under the dump in the lateral and vertical directions.

The object of study

Brief description of the deposit. The Novo-Urskoe deposit was discovered in 1932 in the Ur ore field, which comprises Novo-Urskoe, Beloklyuchevskoe, and Samoilovskoe deposits and several ore occurrences). Within the deposit, 11 orebodies with commercial ores were revealed and explored (Distanov, 1977). The ore field is composed of the dacite porphyry and its tuffs, porphyrites, and quartz–albite–chlorite schists of the Pecherka Formation (pč $Є_1$), occurring among the limestones of the Ancheshevka Formation (an $Є_1$). The rocks dip to the southwest at 60º–70º. The orebodies are composed of massive veinlet-disseminated sulfur–sulfide and sulfide–polymetallic (mostly Cu–Zn) ores. Their structure, morphology, chemical composition, sequence of mineral formation, and exploration history were studied and described by many researchers (Bolgov, 1937; Distanov, 1977; Kovalev, 1969; Zerkalov, 1959, 1962). Following the discovery of the Novo-Urskoe deposit, exploration of its oxidation zone for gold began. The deposit had a typical iron cap with elevated contents of barite and gold. Oxidized orebodies were mined to a depth of 40–50 m. Massive ores were changed by veinlet and, then, disseminated ores in all directions. Massive ores were almost totally composed of sulfides: pyrite, sphalerite, chalcopyrite, fahlores, galena, arsenopyrite, bornite, covellite, and chalcosine. Also, vein minerals were found: quartz, sericite, barite, calcite, and gypsum. Three commercial types of ores were revealed: copper and copper–zinc, zinc, and sulfur–sulfide. Only the upper part of the orebodies, quartz–barite and quartz–pyrite sands, was mined. Extraction of gold from them was performed by cyanidation. The remaining parts of the orebodies stayed intact.

Dumps. The waste of cyanidation of quartz–barite sands (the top, most oxidized part of the orebodies) and quartz–pyrite sands was stored as two dumps without protective constructions or dams in the stream floodplain. The dumps were 10–12 m in height (Fig. 2). Most of the quartz–pyrite sand dump was used for the secondary recovery of barite in the last decade (Fig. 2, left photo). The other dump, from the oxidation zone (Fig. 2, right photo), stayed intact. Over 80 years, the waste was washed out by seasonal rainfall. As a result, the swarmed area downward the tailings storage, up to the Ur River, is covered with an alluvial fan. On the northern side of the dumps, the slope rain and snow runoff gives rise to small ponds drying in the hot season.

Research methods

The given problems are solved using geochemical and geophysical methods. The stream from under the dumps was sampled along its current course. Electrical resistivity to-

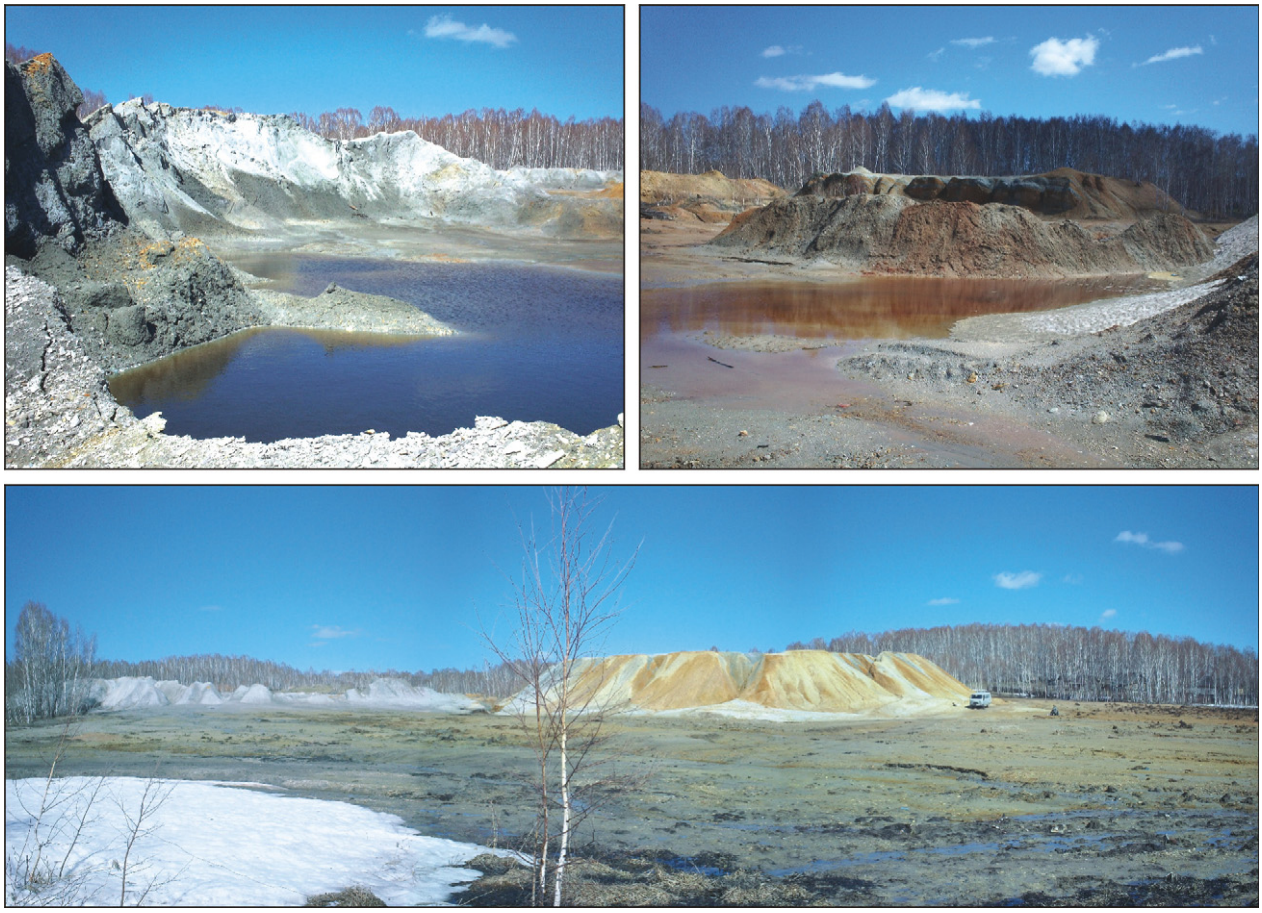

Fig. 2. Appearance of the dump and ponds.

mography studies were performed both at the dump and in the drainage system. Data processing and construction of geoelectrical sections were carried out in the laboratory. The drainage solutions were analyzed for major and trace elements.

Geochemical sampling. Water was sampled from drainage streams (at the sources and along the current), natural stream flowing from the west to the dumps, and ponds in the northern part of the dumps in the spring of 2012. One groundwater sample was taken from a borehole jumped to a depth of ~50 cm. All samples were put into plastic containers. Their pH and Eh were measured in situ with a HI 9125C (HANNA Instruments) pH–Eh-meter. Before the pH measurements, the device was calibrated against standard solutions with known pH values (3.56; 4.01; 6.86; 9.18); the accuracy of measurement was ±0.01 pH. Electric conductivity was measured with a Cond3110 WTW (Wissenschaftlich-Technische Werkstätten GmbH) conductometer, which allows measurements in the range from 0 to 500 mS/cm with an error of ±0.5%. The temperature varied from –5 to +105 °C. The redox potential (Eh) in the samples was also measured with HI 9125C with an accuracy of ±0.01 mV.

The ionic composition of the solutions (SO_4^{2-}, Cl^-, F^-, NO_3^-, NH_4^+, other cations) and trace elements were determined in the laboratory.

Namely, the contents of Cl^-, F^-, NO_3^-, and NH_4^+ were determined by potentiometry on an EKSPERT-001-3.0.4 (Ekoniks-Ekspert) portable ion meter. The accuracy of measurements in the concentration range of 10–500 mg/L was 10%.

The content of SO_4^{2-} was measured by the turbidity method on a PE-5400vi spectrophotometer with an error of 10%.

Major cations (Ca^{2+}, Mg^{2+}, Na^+, K^+) and trace elements were determined by ICP AES on an IRIS Advantage spectrometer at the Analytical Center of the Institute of Geology and Mineralogy, Novosibirsk (analyst S.F. Nechepurenko).

Electrical resistivity tomography (ERT) is a modern modification of the method of vertical electrical sounding (Balkov et al., 2012; Bobachev and Gorbunov, 2005; Loke, 2009). It is one of the resistivity methods based on the Ohm law. Electric current is supplied into the ground via feeding electrodes, and the potential difference is measured on the receiving electrodes. The apparent resistivity of the medium is calculated from the measured voltage and current. ERT is based on multielectrode measurements and automatic 2D data inversion. Inversion means solution of an inverse electrical-survey problem: selection of a model of resistivity distribution in the medium, based on the experimental data. Profile ERT sounding data are interpreted in terms of a 2D model. The results of multielectrode measurements are supplied to the

entrance of a special program, thus forming a geoelectric section: distribution of the electric properties of rocks throughout the depth and along the strike. The ERT data are compared with a priori geological information to make geological interpretation of resistivity sections. During detailed areal works, the results of profile measurements are converted into a 3D array, and 3D data inversion is made. Three-dimensional inversion is appropriate when the object of search is obviously of 3D structure or the geologic environment is rich in three-dimensional inhomogeneities.

Within the study area, ERT sounding was performed along six profiles located at 30 m from each other. The profiles were 355 m in length, and the measurement step was 5 m (Fig. 3). Each profile crossed the entire dump drainage system and ended in the background area (forested zones along the valley edges). Thus, the geologic environment with spreading solutions was fully involved in sounding.

One profile (pr. 0) partly crossed the dump transversely. The dump sounding was performed along the profile with a 2 m step, which ensured more detailed measurements in the section but reduced the depth of research (Khalatov et al., 2013).

The measurements were performed using a SKALA-48 multielectrode electrical-survey station designed in the Laboratory of Electromagnetic Fields of the Institute of Petroleum Geology and Geophysics, Novosibirsk (Balkov et al., 2012), with the sequence of electrode connection corresponding to the Schlumberger setup. Data were processed using the Res2DInv and Res3DInv software (Loke, 2009).

A set of profile data was converted into a 3D array; its quantitative interpretation yielded a 3D geoelectrical model of the medium, whose sections show the depth distribution of resistivity.

Results

Composition of water of temporary ponds. The water samples only partly (at the present moment) reflect the composition of variable pond solutions: During seasonal dump slope runoff, abundant sulfates dissolve; later, in dry weather, they concentrate through evaporation and the additional interaction of water with the underlying waste material. This produces ultra-acidic waters with a wide spectrum of elements, including highly toxic ones (Table 1, prs. UO-1–UO-4). The natural stream curving round the dumps in the west (prs. UR-1 and UR-2) is also strongly contaminated by their sulfide material spread with wind and dissolved in water. The latter has pH ≈ 3; the concentrations of metals (Al, Fe, Co, Ni, Pb, Sr, and Be) are lower than those in the stagnant ponds but are rather high to be considered toxic (Hygienic Standards..., 2003).

Composition of drainage solutions. The drainage flow flooding the entire valley adjacent to the dumps runs from two main sources: In the oxidation zone, the stream flows from under the dump directly at its foot (UO-6, Fig. 3), and near the quartz–pyrite sand dump, the stream (UO-5) originates in the pond formed by seasonal slope runoff. Then the two streams merge. Thus, the samples UO-5 and UO-6 characterize each of the dumps, and the following water samples (Fig. 3, samples 7–15) reflect the cumulative composition.

The stream from the quartz–pyrite sand dump (drainage 1) inherits the characteristics of the pond from which it flows out (UO-1). Naturally, these are the most acidic sulfate–iron waters with pH = 1.92 and mineralization of 7 g/L. Iron cations formed through the dissolution of pyrite amount to 92%, but there are also high concentrations of V, Cr, Cd, and Pb (Table 2). In particular, the concentration of Pb in the

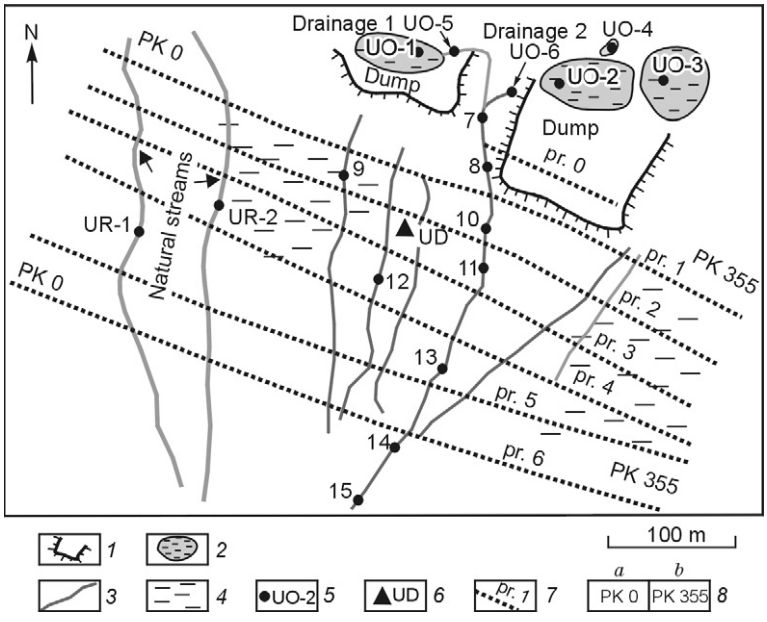

Fig. 3. Scheme of hydrochemical sampling and location of ERT profiles. *1*, dump outlines; *2*, temporary ponds; *3*, drainage and natural streams; *4*, swamped area; *5*, hydrochemical-sampling localities; *6*, groundwater sampling locality; *7*, ERT profiles and their numbers; *8*, beginning (*a*) and end (*b*) of profiles.

Table 1. Physicochemical parameters and element concentrations in the ponds, natural stream, and groundwater

Component	UO-1	UO-2	UO-3	UO-4	UR-1	UR-2	UD
	Ponds				Natural stream		Groundwater
pH	1.67	2.20	2.40	1.95	3.25	2.95	2.70
Eh, mV	674	880	820	654	595	760	790
γ, mS/cm	11.9	7.0	4.1	13.6	0.74	1.2	9.8
SO_4^{2-}, mg/L	9600	5600	2900	35,000	430	510	10,200
Cl^-	0.40	< 3.6	< 3.6	0.40	3.8	18	10
NO_3^-	2.4	0.83	0.61	1.6	4.5	28	2.1
NH_4^+	0.10	1.5	3.4	0.10	0.60	< 0.4	3.8
Ca^{2+}	99	420	430	230	82	110	350
Mg^{2+}	5.6	51	51	420	12	23	310
Na^+	2.4	2.8	8.1	7.9	1.4	8.9	19.3
K^+	9.7	0.31	0.34	5.7	0.48	0.36	< 0.05
SiO_2	13	42	80	78	36	45	210
Fe	2500	1600	300	9800	3.4	4.9	1200
Al	27	180	80	1300	8.9	12	650
Mn	0.78	10	9.6	19	0.95	1.8	49
Cu	4.7	3.2	1.3	12	0.88	0.20	3.3
Zn	1.5	15	13	46	1.2	0.59	35
P	0.18	0.70	0.22	8.8	0.28	0.14	0.82
As	8.6	1.5	0.07	13	< 0.05	< 0.05	< 0.05
Se	0.056	0.33	0.085	4.6	< 0.01	< 0.01	0.29
B	0.020	2.2	0.47	0.072	0.58	< 0.003	5.1
Sr, μg/L	50	340	540	520	540	420	980
Ba	166	66	96	9.5	63	56	48
Li	48	110	84	1400	12	34	1100
V	< 3.0	110	10	< 3.0	< 3.0	< 3.0	90
Cr	< 3.0	< 3.0	70	< 3.0	< 3.0	< 3.0	180
Co	140	210	140	850	18	22	990
Ni	< 3.0	90	60	93	16	26	840
Cd	520	130	36	8.5	< 3.0	< 3.0	140
Be	< 0.3	6.6	2.8	< 0.3	2.2	3.4	42
Pb	2200	410	76	1400	< 30	320	< 30
Sb	200	< 50	< 50	< 50	< 50	< 50	< 50
Ti	660	200	22	1900	< 0.5	< 0.5	20
Zr	110	54	10	420	< 3.0	< 3.0	84
M, g/L	12	7.9	3.9	47	0.58	0.72	13

Note. *M*, Mineralization.

solution is 1.6 mg/L (MPC of Pb is 0.01 mg/L (Hygienic Standards..., 2003)) (MPC is used here just as a reference point).

The drainage waters from under the oxidized dump (UO-6) are acid (pH = 2.55) solutions with mineralization of 2 g/L (Table 2) formed by sulfate anions and a wide spectrum of metal cations (predominantly Al, Fe, and Ca ones). Note that the molar portions of Mn and Zn in these solutions are no more than 1%.

We think that the composition of drainage streams is determined by two main processes: (1) dilution of their water by atmospheric precipitation, which must result in slight neutralization of the solution, and (2) interaction of aggressive acid solutions with the washed-off waste material, dissolution of residual sulfides, and passing of metals into the mobile state. The compositional change of the drainage solutions is seen on the diagrams of element concentrations in the ponds, at the sources of streams, and at the points of their flow down the relief (Fig. 4). At the sources of streams the contents of almost all elements slightly decrease as compared with the ponds (shown by arrows on the diagrams), but in the drainage solutions they increase significantly, with some fluctuations,

Table 2. Physicochemical parameters and composition of water of drainage streams of the Ur dump

Component	Drainage 1 (UO-5)	Drainage 2 (UO-6)	Numbers of sampling localities (Fig. 2)								
			7	8	9	10	11	12	13	14	15
pH	1.92	2.55	2.1	2.2	2.66	2.40	2.2	2.1	2.1	2.1	2.40
Eh, mV	676	810	765	785	711	810	780	786	782	787	820
γ, mS/cm	9.0	2.09	2.07	2.5	1.86	3.19	3.05	3.53	3.88	2.6	4.26
SO_4^{2-}, mg/L	5400	1400	1400	2000	2200	2800	3100	4400	6800	6700	3200
Cl^-	1.2	5.9	0.20	0.40	3.2	6.4	0.50	1.4	2.2	0.40	5.3
NO_3^-	2.6	4.3	1.9	3.3	2.5	12	2.3	2.2	2.5	2.5	11
NH_4^+	0.2	< 0.4	0.5	0.2	0.2	0.5	0.1	0.1	0.2	0.2	0.5
Ca^{2+}	90	180	190	210	190	220	200	220	230	240	220
Mg^{2+}	3.7	38	41	53	58	66	60	73	93	96	77
Na^+	1.0	13	18	19	9.6	12	20	20	20	16	12
K^+	5.2	0.12	0.34	0.28	2.0	0.63	0.33	0.99	0.64	0.56	0.50
SiO_2	8.8	86	82	99	91	93	110	120	100	140	110
Fe	1400	170	280	420	120	380	650	1100	1500	1500	600
Al	17	91	110	160	160	160	190	240	310	310	206
Mn	0.55	8.1	7.7	11	9.2	11	13	15	18	16	13
Cu	2.5	1.1	1.5	1.9	2.3	1.8	2.2	2.8	3.4	3.4	2.0
Zn	0.96	10	16	18	16	9.8	17	18	20	21	12
P	0.25	0.36	0.16	0.17	0.22	0.42	0.66	1.4	1.7	2.5	0.52
As	4.1	< 0.05	< 0.05	< 0.05	< 0.05	< 0.05	0.20	1.1	1.7	1.1	< 0.05
Se	1.8	0.082	< 0.01	0.28	0.074	0.12	0.89	1.7	2.0	1.3	0.20
B	0.053	0.070	0.83	0.49	0.11	0.40	0.85	1.7	2.7	4.3	0.84
Sr, μg/L	71	410	450	530	430	630	530	590	600	600	570
Ba	100	40	21	20	10	130	14	13	9.0	9.0	78
Li	51	67	100	130	160	120	170	210	270	250	160
V	77	16	< 3.0	380	10	24	350	440	300	600	44
Cr	52		15	13	20	26	33	96	120	200	0
Co	56	120	51	110	130	160	140	170	230	320	190
Ni	< 3.0	59	21	150	70	68	180	220	240	330	72
Cd	270	25	39	30	60	36	48	83	130	200	52
Pb	1600	< 30	65	130	140	72	91	210	220	320	80
Be	< 0.3	4.2	< 0.3	7.7	< 0.3	5.8	7.8	9.3	6.3	20	6.4
Sb	< 50	72	< 50	< 50	< 50	< 50	< 50	< 50	< 50	< 50	< 50
Ti	280	< 0.5	< 0.5	18	16	44	99	440	360	500	56
Zr	68	< 3.0	< 3.0	66	13	16	80	110	130	96	16
M, g/L	2.0	6.9	2.1	3.0	2.8	3.7	4.3	6.1	9.1	9.1	4.5

since the acidic medium favors the transition of metals from the mechanically dispersed waste material into the solutions. At a first glance, it seems unlikely that the concentrations of metals increase with distance from the dump and the pH of water does not increase for a long time. This means that the buffer capacity of the studied system is almost exhausted. A slight decrease in metal concentrations begins only at 1 km from the dumps, though they remain extremely high.

As follows from the water composition, the acidic medium causes not only dissolution of secondary sulfates and residual sulfides but also disintegration of the waste rock matrix. It is believed that technogenic processes lead to a decrease in the portion of metals and an increase in the portion of rock-forming elements in water. Several associations of elements are recognized according to their correlation coefficients, which reflect both their initial relationships in the ore-rock mixture and the new ones caused by a hypergene change of the dump (Table 3). The high coefficients of correlation between dissolved element species of silicate oxides (SiO_2–Al_2O_3–CaO–MgO–MnO–SrO) testify to the active removal of rock-forming and trace elements (Li, Be, V, P, Cr, Co) from the vein waste:

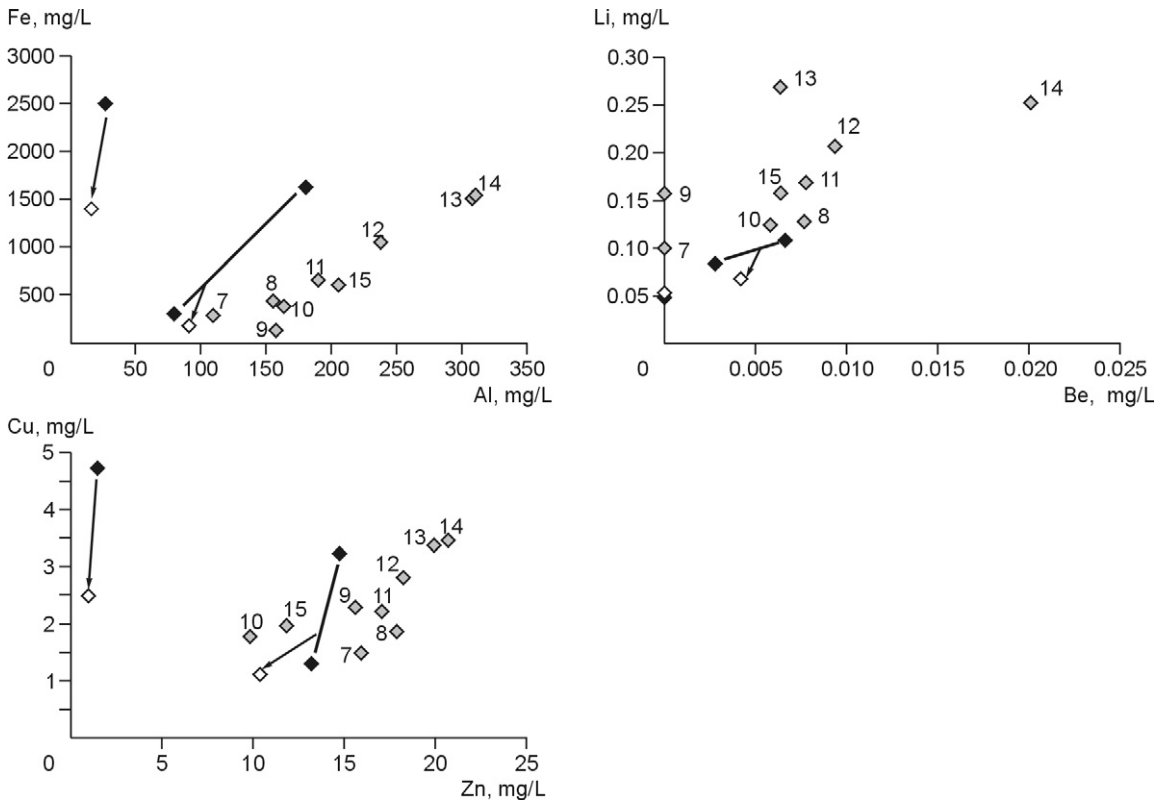

Fig. 4. Changes in concentrations of some elements in the drainage streams from the dumps in comparison with their initial concentrations in the ponds. Black rhombuses mark ponds; white rhombuses, the sources of streams; and gray rhombuses, the drainage streams; 7–15, sampling points along the current course.

(1) Ca-Si-Al-Mn-Li association is specific for albitophyres composing most of the metamorphic rocks hosting the Novo-Urskoe deposit;

(2) Mg–Ni–Co–Cr–V association was, most likely, leached from gabbro-diabases widespread in the Ur ore filed;

(3) Ca–Sr association was obviously extracted from the Lower Cambrian limestones of the Gavrilovka Formation.

The Fe-Pb-Zn-Cd-As-Se ore association in the drainage stream follows the regularities of migration in acidic high-sulfate medium. For example, the negative Zn-Ba and Zn-Pb

Table 3. Correlation matrix of elements in acid drainage solutions, n = 11

Component	Ca	Mg	SiO_2	Fe	Al	Mn	Cu	Zn	Sr	Ba	Li	Cd	Be	P	As	Pb
Mg	**0.923**															
SiO_2	**0.940**	**0.889**														
Fe	–0.008	0.292	0.042													
Al	**0.857**	**0.973**	**0.854**	0.459												
Mn	**0.930**	**0.960**	**0.896**	0.270	**0.959**											
Cu	0.267	0.560	0.319	***0.706***	***0.706***	0.518										
Zn	**0.829**	**0.770**	**0.863**	0.101	**0.808**	**0.834**	0.417									
Sr	**0.985**	**0.888**	**0.905**	–0.055	**0.809**	**0.911**	0.200	**0.761**								
Ba	–0.398	–0.374	–0.540	–0.075	–0.478	–0.473	–0.331	**–0.821**	–0.294							
Li	**0.754**	**0.914**	**0.761**	0.544	**0.977**	**0.904**	**0.812**	**0.794**	***0.697***	–0.536						
Cd	–0.461	–0.147	–0.363	**0.834**	0.005	–0.244	***0.658***	–0.301	–0.519	0.141	0.125					
Be	0.634	***0.702***	**0.761**	0.499	**0.746**	0.191	0.557	0.564	0.587	–0.288	***0.670***	0.191				
P	0.528	**0.739**	***0.633***	***0.760***	**0.837**	**0.827**	**0.838**	0.572	0.466	–0.397	**0.846**	0.441	**0.827**			
As	***–0.637***	–0.361	–0.599	***0.756***	–0.198	**0.821**	0.509	–0.469	–0.653	0.243	–0.059	**0.912**	–0.082	0.212		
Pb	**–0.799**	–0.574	***–0.749***	0.554	–0.444	**0.939**	0.291	***–0.651***	**–0.810**	0.388	–0.316	**0.863**	–0.213	–0.041	**0.939**	
Se	–0.110	0.169	–0.061	**0.922**	0.362	0.559	**0.825**	0.082	–0.129	–0.157	0.486	**0.741**	0.307	***0.638***	**0.791**	0.559

Note. Bold-typed are values of $r > r_{01}$, italic bold-typed are values of $r_{01} > r > r_{05}$; r, correlation coefficient.

Table 4. Element species in acid sulfate solutions at pH = 1.7

Fe, Al	Mol. %	As	Mol. %	Zn, Cu	Mol. %
$FeSO_4$	62.3	H_3AsO_4	8.4	Zn^{++}	38.6
$Fe(SO_4)^{2-}$	21.2	$FeAsO_4$	6.0	$ZnSO_4$	39.6
$FeHSO_4^{++}$	9.0	$FeHAsO_4^+$	41.0	$Zn(SO_4)_2^-$	21.9
Fe^{+++}	7.5	$FeH_2AsO_4^{++}$	44.0	Cu^{++}	52.8
Al^{+++}	8.4	$AlHAsO_4^+$	0.3	$CuSO_4$	47.2
$AlSO_4^+$	60.3	$MgH_2AsO_4^+$	0.3	Mn^{++}	50.3
$Al(SO_4)^{2-}$	31.2	$CaH_2AsO_4^+$	0.0	$MnSO_4$	49.7

correlation coefficients (despite the coexistence of sphalerite, galena, and barite in the ores) are due to the contrasting geochemical properties of these elements: Formation of virtually insoluble barite ($BaSO_4$) and anglesite ($PbSO_4$) favors extraction of Ba and Pb from the solutions, whereas zinc sulfate complexes remain migratory. Moreover, the drainage streams contain soluble gold supplied from the waste. Its behavior under interaction of the stream water with the swamp matter was thoroughly studied earlier (Myagkaya et al., 2013).

A highly toxic element Be requires a special discussion. Its electrochemical behavior is just briefly reviewed in literature, whereas it is often present in high concentrations in acid drainage streams (Bortnikova et al., 2011). Beryllium is characterized by an isomorphic incorporation into various rock-forming minerals (Ivanov, 1993). It is, most likely, extracted from sericite, Na-plagioclase, quartz-sericite schists, and albitophyres of the Pecherka Formation and is therefore correlated with a wide range of elements. In the kinetic experiments (Bortnikova et al., 2010), Be appeared in drainage solutions after Li and Al during the acidification of the medium to pH = 4.42 as a result of the destruction of muscovite–sericite micas. Note that in sulfate drainage solutions this element remains mobile and can be transported to remote distances in the absence of hydrochemical barriers (Ivanov, 1993).

Special attention should be paid to groundwater (sample UD). The repeated dissolution of sulfides, deposition and dissolution of sulfates, and leaching of rock-forming and ore minerals lead to the formation of a vertical anomaly under the action of infiltration gravity water within the drainage area. At a depth of ~50 cm, we found the highest concentrations of sulfates, Al (650 mg/L), Li (1100 μg/L), Cr (180 μg/L), and Be (42 μg/L). Detection of such high concentrations of elements in groundwater was an additional argument for geophysical research aimed at tracing the true contours of this anomaly.

Element species in the drainage solutions. Based on the results of physicochemical modeling with the use of the HCh software (Shvarov, 1999), we detected element species in the acid drainage solutions and estimated the under- and oversaturation of the latter with these elements relative to some minerals. The calculations were made using the compositions of drainage solutions (Table 2) and the water from the pond near a primary-ore dump (pH = 1.67).

At pH = 1.67, jarosite, barite, and quartz can be deposited (the solutions are in equilibrium with gypsum), and at pH = 2.6, only quartz and barite were observed. Formation of exotic minerals bukovskyite $Fe_2(AsO_4)(SO_4)(OH)\cdot 7H_2O$ and conichalcite $CaCuAsO_4(OH)$ as a result of high concentrations of As (up to 13 mg/L) in the solutions is not ruled out either (Gas'kova et al., 2008). Various cations and As species in the solutions with pH = 1.67 are listed in Table 4. It is obvious that 92.5% Fe and 91.5% Al are bounded in sulfate complexes. Therefore, the solid phase lacks their oxides and hydroxides capable to adsorb toxic cations of heavy metals and As. Jarosite is produced, but it has a lower sorption capacity for

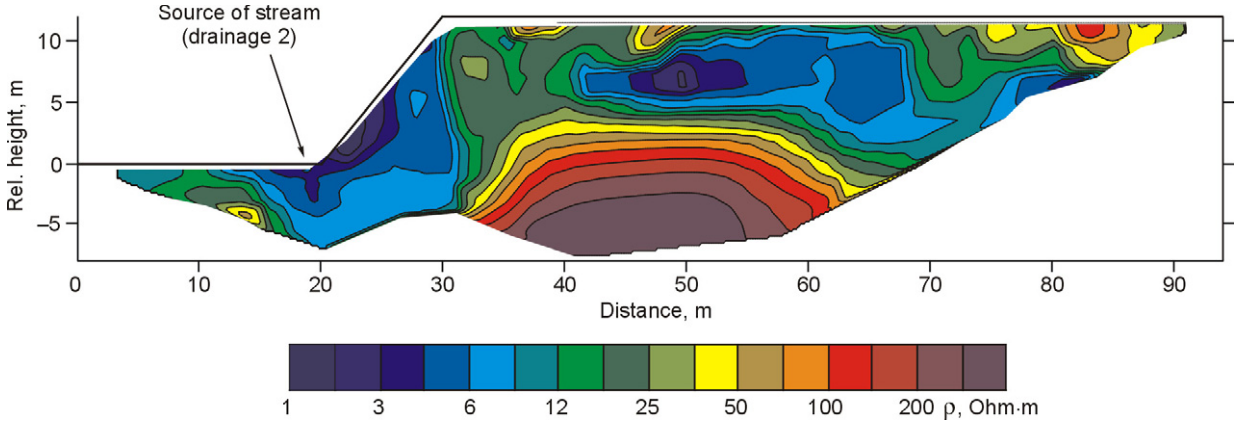

Fig. 5. Resistivity distribution throughout the dump section (pr. 0).

As (Asta et al., 2010). Note that according to the calculation results, more than 90% of As are present as iron arsenate complexes, and the portion of sulfate complexes of Mn, Cu, and Zn reaches 50%. A large amount of hydroxides, imparting a specific sandy-brown color to the valley deposits, is produced as a result of neutralization of the solutions through their reactions with vein minerals or soil organics or as a result of their dilution and subsequent evaporation during seasonal temperature and hydrological-regime fluctuations. For example, model calculations showed that as pH increases to 3.6, ferrihydrite amounts to ~60% of the solid phase (the portion of jarosite is <40%); at pH = 4.2, gibbsite and kaolinite appear (3.7 and 7.1%, respectively). Aluminum dominates over iron in the solutions (drainage 2) when intense deposition of oxides and hydroxides of Fe(III) takes place. Earlier we reported that soils around piled dumps are always enriched in heavy metals; iron and copper are most firmly bound with organic material, and zinc concentrates in the mobile fraction of soil extracts (Gaskova et al., 2012; Novikova and Gas'kova, 2013).

Vertical and lateral distribution of the drainage solutions. Figure 5 shows the distribution of resistivity (ρ) throughout the dump section. It varies from 1.3 to 25.0 Ohm·m. In the bottom of the section, there is a high-resistivity anomaly caused by the close occurrence of bedrocks in the dump base, which are exposed in the stream bed. The

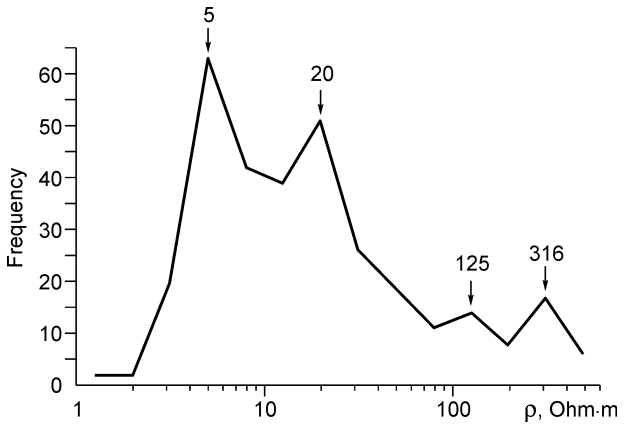

Fig. 6. Statistical distribution resistivity of tailings in the dump. The numerals above the curve show modal resistivity values (Ohm·m).

wide interval of ρ values in the tailings is probably due to the nonuniform invasion of solutions into the dump body.

Statistical analysis showed that the ρ distribution throughout the dump section is multimodal (Fig. 6). The bulk of the dump is characterized by modal values ρ = 5 and 20 Ohm·m. The minimum ρ value is probably specific for areas saturated with highly mineralized acid solutions. According to the known dependence of resistivity on the total mineralization

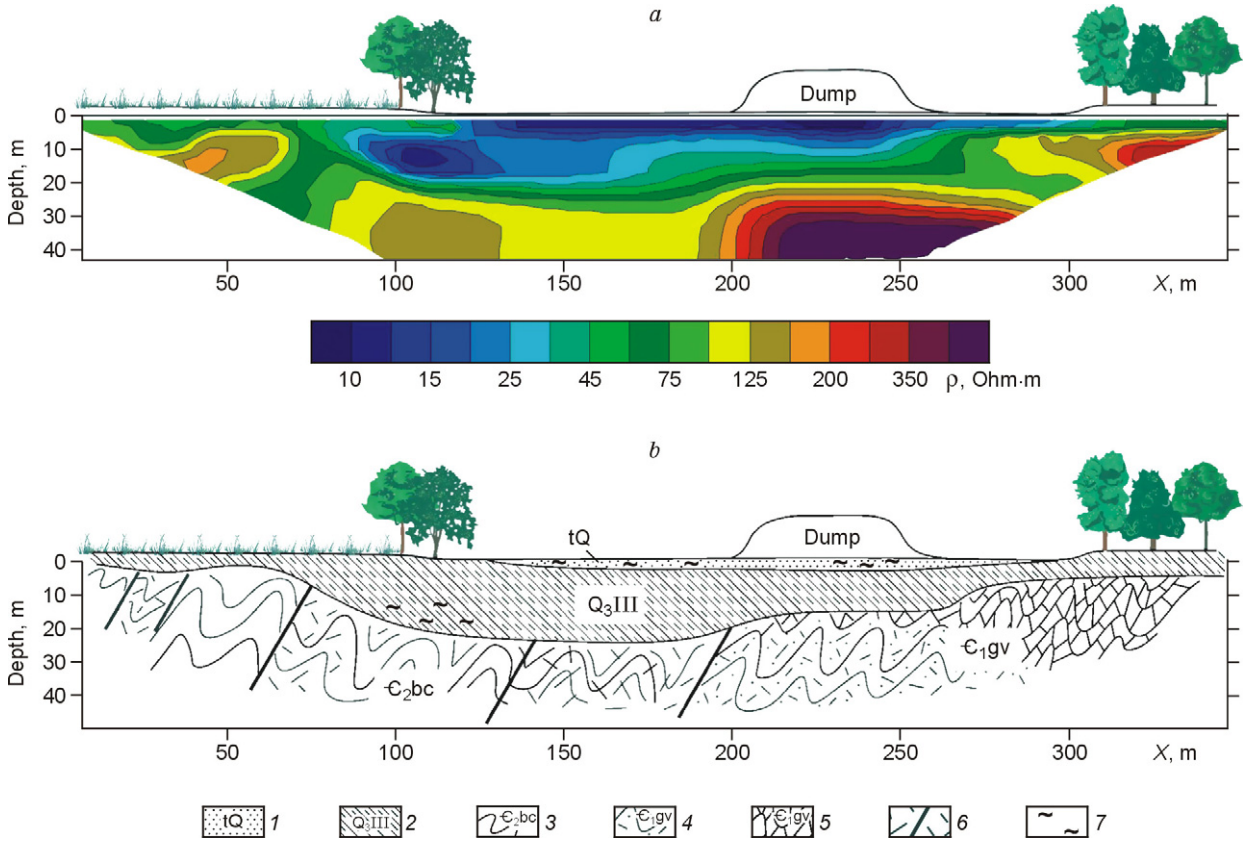

Fig. 7. Geoelectrical section along profile 1 (*a*) and its interpretation (*b*). *1*, technogenic deposits; *2*, Quaternary alluvial loess-like loams; *3*, clay–chlorite schists and siltstones of the Middle Cambrian Bachat Formation; *4*, tuffs of the Lower Cambrian Gavrilovka Formation; *5*, limestones of the Lower Cambrian Gavrilovka Formation; *6*, faults and fractured zones; *7*, groundwater contaminated by acid solutions.

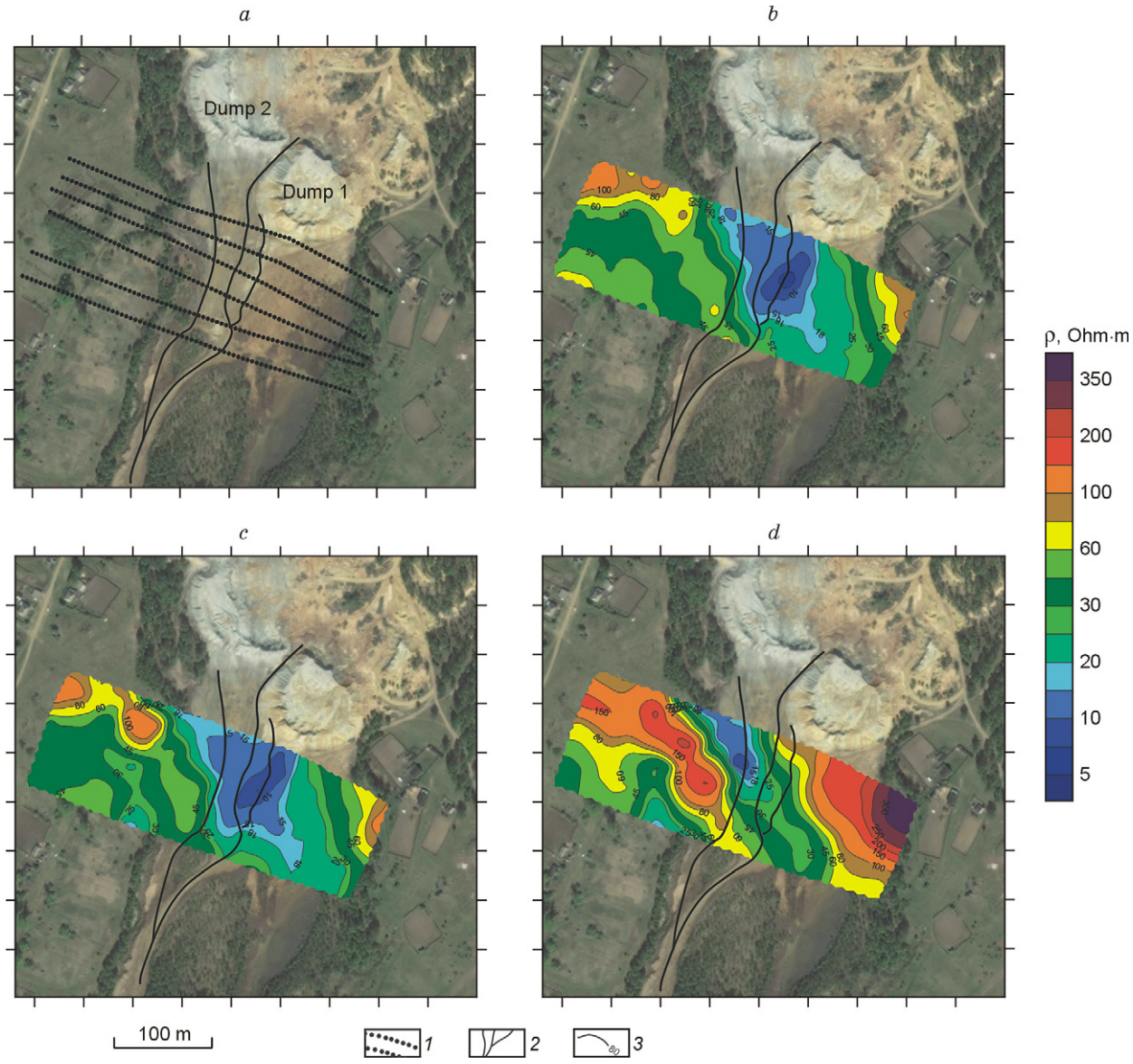

Fig. 8. Satellite image of the study area (*a*) and map of resistivity distribution at depths of 1.25 m (*b*), 7 m (*c*), and 15 m (*d*). *1*, ERT profiles; *2*, streams; *3*, resistivity isolines.

(SP 11-105-97..., 2004), ρ = 5 Ohm·m of sandy loam and loam (the waste contains a large amount of clay fraction formed in the hypergenesis zone of the deposit; therefore, it can be approximately called loams) corresponds to pore water mineralization of 12.5 g/L. According to the data of geochemical sampling, the groundwater mineralization in the dump bottom is 13 g/L (sample UD, Table 1). The dump material with ρ = 20 Ohm·m is apparently low-water tailings. We think that the nonuniform invasion of solutions into the dump body is due to the so-called channel filtration, known as heap leaching, i.e., invasion of solutions into an ore pile along the same channels (Fazlullin, 2001).

Figure 7 shows a geoelectrical section along profile 1 passing near the dump and its interpretation taking into account known geological information (Bessonenko and Kuznetsov, 1970). In the section bottom, there are bedrocks with high resistivity: schists (50–120 Ohm·m), tuffs (200–500 Ohm·m), and limestones (100–300 Ohm·m). The sites with low ρ values are crush and schistosity zones. The Quaternary deposits of the stream bed (loess-like loams and sands) are characterized by low ρ (15–30 Ohm·m). The section top in the stream bed, composed of technogenic sands (dump fan), exhibits the lowest ρ values (8–10 Ohm·m), which might be associated with the contamination of groundwater by acid solutions. The minimum ρ value (8 Ohm·m) is detected at depths of 1.25–2.50 m, in the bottom of the dump with a drainage stream. The resistivity of 7–10 Ohm·m of loams corresponds to pore water mineralization of ~2 g/L (SP 11-105-97..., 2004). Thus, penetration of solutions into the section leads to their impoverishment by groundwater and a six-fold decrease in mineralization.

The ρ distribution in plan helps to elucidate the direction of flow of acid solutions and assess the scales of environmental pollution. Figure 8 shows a satellite image of the study

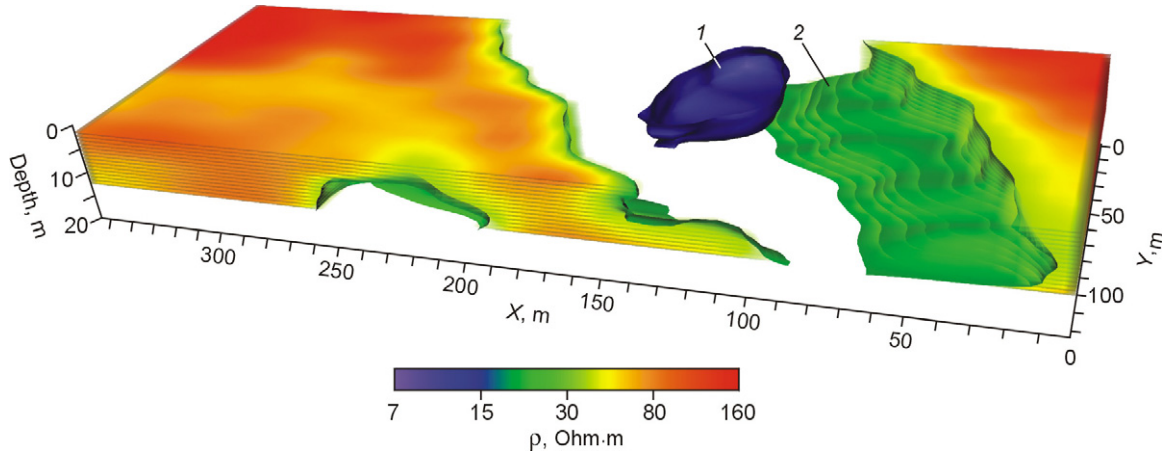

Fig. 9. Three-dimensional geoelectrical model of the study area. Isosurfaces: *1*, 11 Ohm·m; *2*, 30 Ohm·m.

area and maps of ρ distribution at depths of 1.25, 7, and 15 m. On the map of ρ distribution at a depth of 1.25 m, floodplain deposits are recognized as an S-SE striking zone of low resistivity (15–30 Ohm·m). In this zone, a local intense low-ρ (5–10 Ohm·m) anomaly of S-SW strike maps a flow of acid solutions filtered from under the dump (drainage 1). Low-resistivity anomaly is also traceable at a depth of 7 m (Fig. 8*c*), which suggests a rather deep invasion of the solutions into the floodplain deposits.

On the map of ρ distribution at a depth of 15 m, a narrow (~40 m) linear low-ρ area of S-Se strike is revealed, interpreted as a fault zone. The fault zones are usually groundwater reservoirs. The low-resistivity (5–15 Ohm·m) anomaly in the fault located at a slightly lower hypsometric level than dump 2 might be due to contamination of fracture–vein waters of the fault by acid drainage solutions. Thus, the ERT-detected fault might serve as a reservoir ensuring the long-distance spreading of geochemical contamination.

Figure 9 shows a three-dimensional geoelectrical model of the study area (the view from the dumps along the stream valley). The 11 Ohm·m isosurface shows the area of surficial contamination of soil by acid solutions, and the 30 Ohm·m isosurface outlines the fault zone.

The performed geophysical research has revealed two types of contamination within the study area. The first type is contamination of the surface runoff by acid drainage solutions percolating to a depth of 10 m and filtered in the S-SW direction, concordantly to the strike of the stream valley. The second type is deep contamination, i.e., penetration of acid solutions into the fracture-vein waters of the S-SE striking fault.

Conclusions

(1) The drainage streams from the Ur dump of cyanided oxidized and primary ores are highly mineralized (up to 13 g/L) acid solutions with extremely high concentrations of toxic elements, which are produced under interaction of the dump substance with pore waters and seasonal streams. Concentrations of elements do not decrease in the drainage streams for at least 1 km because of the intense secondary leaching of the solid dump waste by acid solutions.

(2) The major species in the drainage stream water are sulfate and arsenate complexes; manganese, copper, and zinc are present as aqua ions as well. The intense complexation maintains constant concentrations of elements in the solution at the long distance from the dumps and prevents precipitation of secondary phases. The calculations have shown the necessity of neutralization barriers, which will help to remove a considerable portion of toxic elements, e.g., through their coprecipitation with oxides and hydroxides of Fe and Al.

(3) The vertical spreading of the drainage solutions is of two types: surficial valley slope runoff and percolation through weakened fault zones to a depth of 20 m.

(4) The geophysical data suggest that the invasion of drainage solutions into the ground results in their dilution with pure groundwater, leading to a six-fold decrease in total mineralization.

We thank O.P. Saeva and A.Yu. Devyatova for participation in the field sampling, E.O. Rybkina for analyses, and S.Yu. Khalatov and E.V. Balkov for help with field research and for provided geophysical data.

This work was supported by research project 01201351721 from the Institute of Petroleum Geology and Geophysics, Novosibirsk, and by grants 14-05-00293 and 14-05-31396 from the Russian Foundation for Basic Research.

References

Asta, M.P., Ayora, C., Román-Ross, G., Cama, J., Acero, P., Gault, A.G., Charnock, J.M., Bardelli, F., 2010. Natural attenuation of arsenic in the Tinto Santa Rosa acid stream (Iberian Pyritic Belt, SW Spain): The role of iron precipitates. Chem. Geol. 271, 1–12.

Ayolabi, E.A., Folorunso, A.F., Kayode, O.T., 2013. Integrated geophysical and geochemical methods for environmental assessment of municipal dumpsite system. Int. J. Geosci. 4, 850–862.

Balkov, E.V., Panin, G.L., Manshtein, Yu.A., Manshtein, A.K., Beloborodov, V.A., 2012. Electrotomography: equipment, technique, and application. Geofizika, No. 6, 54–63.

Bessonenko, V.V., Kuznetsov, A.M., 1970. Geological Map of the USSR. Scale 1:200,000. Kuzbass Series. Sheet N-45-XIV. Explanatory Note [in Russian]. Nedra, Moscow.

Blair, R.D., Cherry, J.A., Lim, T.P., Vivyurka, A.J., 1980. Groundwater monitoring and contaminant occurrence at an abandoned tailings area, Eliot Lake, Ontario, in: Proc. 1st Int. Conf. Uranium Mine Waste Disposal, Vancouver, May 19–21. Soc. Min. Eng., Am. Inst. Min. Eng., New York, pp. 411–444.

Bobachev, A.A., Gorbunov, A.A., 2005. Two-dimensional electric resistivity and induced polarization survey: equipment, technique, and software. Razvedka i Okhrana Nedr, No. 12, 52–54.

Bolgov, G.P., 1937. Salair sulfides. The Ur polymetallic deposits. Izv. Tomskogo Industrial'nogo Instituta 58 (3), 45–96.

Boorman, R.S., Watson, D.M., 1976. Chemical processes in abandoned sulfide tailings dumps and environmental implications for Northeastern New Brunswick. Can. Inst. Mining Metall. Bull. 69, 86–96.

Bortnikova, S.B., Gaskova, O.L., Prisekina, N.A., 2010. Geochemical estimation of the potential danger of waste rocks from the Veduginskoe deposit. Geochem. Int. 48 (3), 280–294.

Bortnikova, S., Manstein, Yu., Saeva, O., Yurkevich, N., Gaskova, O., Bessonova, E., Romanov, R., Ermolaeva, N., Chernuhin, V., Reutsky, A., 2011. Acid mine drainage migration of Belovo Zinc Plant (South Siberia, Russia): A multidisciplinary study, in: Scozzari, A., Mansouri, B. (Eds.), Water Security in the Mediterranean Region. An International Evaluation of Management, Control, and Governance Approaches. Springer, Dordrecht, pp. 191–208.

Distanov, E.G., 1977. Pyrite-Polymetallic Deposits of Siberia [in Russian]. Nauka, Novosibirsk.

Fazlullin, M.I. (Ed.), 2001. Heap Leaching of Noble Metals [in Russian]. Izd. Akademii Gornykh Nauk, Moscow.

Gas'kova, O.L., Shironosova, G.P., Bortnikova, S.B., 2008. Thermodynamic estimation of the stability field of bukovskyite, an iron sulfoarsenate. Geochem. Int. 46 (1), 85–91.

Gaskova, O.L., Bortnikova, S.B., Kabannik, V.G., Novikova, S.P., 2012. Features of soil pollution in the region of storage of the wastes from pyrometallurgical zinc extraction at the Belovo Zinc Plant. Chemistry for Sustainable Development, No. 4, 375–384.

Hygienic Standards GN 2.1.5.1315-03 "Maximum Permissible Concentrations (MPC) of Chemicals in Water Objects of Household and Social Use" [in Russian], 2003. Minyust RF, Moscow. http:.docs.cntd.ru/document/901862249.

Ivanov, V.V., 1993. Ecological Geochemistry of Elements [in Russian]. Nedra, Moscow, Vol. 1.

Kargar, M., Khorasani, N., Karami, M., Rafiee, G.H., Naseh, R., 2012. Statistical source identification of major and trace elements in groundwater downward the tailings dam of Miduk Copper Complex, Kerman, Iran. Environ. Monit. Assess. 184 (10), 6173–6185.

Khalatov, S.Yu., Balkov, E.V., Bortnikova, S.B., Saeva, O.P., Korneeva, T.V., 2013. Geoelectrical methods of study of mining dumps, in: Engineering Geophysics 2013. The Ninth International Conference and Exhibition (Gelendzhik, 22–26 April 2013) [in Russian], p. E15.

Kovalev, K.R., 1969. Specifics of Ore Formation at Pyrite-Polymetallic Deposits of Northeastern Salair and Eastern Tuva. PhD Thesis [in Russian]. NGU, Novosibirsk.

Loke, M.H., 2009. Electrical Imaging Surveys for Environmental and Engineering Studies. A Practical Guide to 2-D and 3-D Surveys, RES2DINV Manual, IRIS Instruments, www.iris-instruments.com.

Myagkaya, I.N., Lazareva, E.V., Gustaitis, M.A., Zayakina, S.B., Polyakova, E.V., Zhmodik, S.M., 2013. Gold in the sulfide waste–peat bog system as a behavior model in geological processes. Dokl. Earth Sci. 453 (1), 1132–1136.

Novikova, S.P., Gas'kova, O.L., 2013. Influence of natural fulvic acids on the solubility of sulfide ores (experimental study). Russian Geology and Geophysics (Geologiya i Geofizika) 54 (5), 509–517 (665–675).

Olias, M., Moral, F., Galvan, L., Ceron, J.C., 2012. Groundwater contamination evolution in the Guadiamar and Agrio aquifers after the Aznalcollar spill: assessment and environmental implications. Environ. Monit. Assess. 184 (6), 3629–3641.

Sainz, A., Grande, J.A., de la Torre, M.L., 2004. Characterisation of heavy metal discharge into the Ria of Huelva. Environ. Int. 30 (4), 557–566.

Shvarov, Yu.V., 1999. Algorithmization of numerical equilibrium simulation of dynamic geochemical processes. Geokhimiya, No. 6, 646–652.

SP 11-105-97. Engineering Geological Investigations for Construction. Part 6. Rules of Carrying Out Geophysical Investigations [in Russian], 2004. PNIIIS Gosstroya Rossii, Moscow.

Spiridonov, A.M., Zorina, L.D., Romanov, V.A., 2014. Types of endogenous geochemical fields and their significance for prospecting. Russian Geology and Geophysics (Geologiya i Geofizika) 55 (2), 290–298 (370–380).

Yuval, Oldenburg, D.W., 1996. DC resistivity and IP methods in acid mine drainage problems: results from the Copper Cliff mine tailings impoundments. J. Appl. Geophys. 34, 187–198.

Zerkalov, V.I., 1959. New minerals in ores of the Ur deposits, Salair. Vestnik Zapadno-Sibirskogo i Novosibirskogo Geologicheskogo Upravleniya, Issue 4, 57–59.

Zerkalov, V.I., 1962. Mineralogy and Geology of Cu–Pb–Zn Pyrite Deposits of Northeastern Salair. PhD Thesis [in Russian]. TPI, Tomsk.

Editorial responsibility: M.I. Epov